Journal of Engineering Science and Technology
Vol. 4, No. 1 (2009) 1 - 19

ROLLING PROCESS WITH OHSAS AND TEXTURE FORMATION– A REVIEW

P. CHANDRAMOHAN[1*], K. MANIKANDA SUBRAMANIAN[1],
P. CHANDRASEKAR[2,]

[1]Sri Krishna college of Engineering and Technology, Coimbatore-641008, Tamilnadu, India.
[2]Swinburne Univ. of Technology (Sarawak Campus), Malaysia.
*Corresponding Author: pcmohu@yahoo.co.in

Abstract

Rolling is a mechanical treatment, which plays an important part in the processing of ferrous and nonferrous alloys. Texturing is an important phenomenon that occurs after rolling process. Preferred orientation increases the strength of the material enormously. Hence the research is focused on the rolling studies and the texture formation, which occurs after rolling process. This review mainly focuses on rolling process carried out in different alloys. It also highlights the analysis made on various rolling parameters for improving the mechanical properties. Texture studies carried on various ferrous and non-ferrous alloys; particularly in nitrogen alloyed duplex stainless steel is discussed. Finally the need for implementation of occupational health and safety during a thermomechanical treatment is also discussed. The state of art in this field is encouraging and showing positive signs of commercializing rolled nitrogen alloyed duplex stainless steel after proper texture control.

Keywords: Rolling, Texture, Duplex, Recrystallization, Fibre.

1. Rolling Studies

Thermomechanical treatment involves the simultaneous application of heat and a deformation process to an alloy, in order to change its shape, modify the microstructure and develop texture. Hot rolling of metals is a common thermomechanical treatment, which plays an important part in the processing of various compositions of many steels ranging from low carbon, mild steels to highly alloyed stainless steels. The traditional fabrication route involves the casting of ingots varying in size from 1 to 50 tonnes, which are soaked at very

Nomenclatures

DSS	Duplex Stainless Steel
FDM	Finite Difference Method
FEM	Finite Element Method
H_m	Mean Thickness
IF	Interstitial Free
IPF	Inverse Pole Figures
K_b	Boltzmann constant
L	Contact Length
MC	Monte Carlo Simulations
MDF	Misorientation Distribution Function
$\langle m_{ij} \rangle$	Effective mobilities between i recrystallizing texture components and j deformation texture components
ND	Normal Direction
N_{ij}	Number of newly formed nuclei belonging to the recrystallizing texture component i growing within the deformation texture component j
$\langle N_{ij} \rangle$	Corresponding equivalent nucleation rate which may assume any form desired.
ODF	Orientation Distribution Function
OHSAS	Occupational Health And Safety Management System
PAH	Polycyclic Aromatic Hydrocarbons
PB	Phase Boundaries
P_j	Function of the deformed orientation component of the total plastic strain and of time
Q_{ij}	Activation Energy Matrix
$\langle r_{ij} \rangle$	Equivalent radius of the recrystallizing texture component i growing within the deformation texture component j.
SIR	Standardized Incidence Ratio
T	Absolute temperature
TOF	Time-of-flight
X_j^{def}	Remaining volume fraction of the deformed texture component
XRD	X-ray Diffraction

Greek Symbols

β	Beta fibre
$\langle \Delta r_{ij} \rangle$	Increase in the equivalent radius of the recrystallizing texture component during the time step Δt
$\Delta V_{ij}^{\exp}$	Difference matrix form for the expanded volume
ΔV_{ij}^{RX}	Deformation volume for the recrystallized fraction

Subscripts and Superscripts

def	Deformed
exp	Exponential
i	Recrystallizing texture component
j	Deformation texture component
o	Initial

high temperatures (1200-1300°C) and then progressively hot rolled to billets, bars and sheet. This leads to the refining of the original coarse cast structure by repeated recrystallization of the steel while in the austenitic condition, and by the gradual reduction of inhomogenities of composition caused by segregation during casting. Also, the inevitable non-metallic inclusions, i.e. oxides, silicates, sulphides, are broken up, some deformed, and distributed throughout the steel in a more uniform manner [1-4].

Rolled products can be divided into foil, sheet and plate. Thickness of the foil is less than 0.2 mm and is used mainly in the packaging industry for foil containers and wrapping. Foil is also used for electrical applications, building insulation and in the printing industry. Thickness of the sheet ranges from 0.2 mm to 6 mm and has a wide variety of uses in the construction industry including aluminium siding and roofing. Sheet is also used extensively in transport applications such as automobile body panels, airframes and the hulls of boats. Plate is any rolled product, which is over 6 mm in thickness. Its application includes airframes, military vehicles and structural components in bridges and buildings [5-8].

Some important parameters that influence properties of the rolled product include rolling temperature, the rolling speed, the roll temperature, friction and the ratio of the mean thickness to the contact length in the roll gap. Among the above said parameters, rolling temperature has the greatest influence, whereas the roll temperature and roll speed have little influence on the microstructure and specifically on the volume fraction recrystallized [9].

Prediction of width variation (spread) either by analytical or the numerical methods during the breakdown passes in the commercial hot flat rolling of aluminium alloys is essential. All existing empirical formulae are constructed from the regression analysis of laboratory experimental data [10-11]. The formulae are only valid for a limited range of rolling conditions. A new formula was developed by T. Sheppard and X. Duan by the introduction of the factor H_m/L, i.e. mean thickness to contact length in the roll gap [12].

An approach to develop the technology for rolling strips from copper and its alloys on four high rolling mills was investigated by Z. Rdzawsky and Sadkowski A. [13]. The investigations carried out were aimed at taking full advantage of the rolling mill power to produce strips of required quality. In order to develop correct rolling technology it is essential to analyze thoroughly the forces present during rolling. Morawiecki's formula has been used in calculating the roll force [13]. To perform calculation of the rolling scheme properly it is important to determine the yield stress changes during rolling, since the yield stress essentially affects the rolling force. Results of investigations presented in this work show the possibilities of further modernization of the strips rolling technology. The approach makes possible taking full advantage of the rolling mill power and possibilities of deformation of the material rolled. The investigations showed that it is very difficult to develop a formula which is sufficiently accurate and at the same time universally applicable computational formula to describe all the rolling process. Instead, an individual approach applicable to each rolling mill and to each material being rolled on that mill is recommended [13].

2. Texture Studies in Nonferrous Alloys

Texture evolution of continuous cast and direct chill cast aluminium alloys were studied after cold rolling by W.C. Liu et al. [14]. The continuous cast and direct chill cast hot bands possessed a typical deformed structure and a strong β fiber rolling texture. In order to generate a fully recrystallized microstructure prior to cold rolling the continuous cast and direct chill cast hot bands were annealed and then water quenched. The recrystallization texture of the continuous by cast hot band was completely different from that of the direct chill cast hot band. The recrystallization texture of the continuous cast hot band consisted of the 45^{o} ND rotated cube component with a strong scattering towards the {1 1 5} < 1 1 0 > orientation, while The recrystallization texture of the direct chill cast hot band was characterized by a strong cube orientation {0 0 1} < 1 0 0 > and a minor *P* orientation {1 1 0} < 5 5 4 >.

The processing method has a strong influence on the texture evolution during rolling. Continuous cast aluminium alloy exhibits a higher rate of formation of the β fiber component than direct chill cast aluminium alloy [14]. The volume fractions of texture components can be calculated by an improved integration method [15-17].

The rolling texture of heavily rolled pure Nickel has been found to be similar to the rolling texture of deformed pure Copper. The textures of Ni-Fe alloys with up to 40% Fe are similar amongst themselves and also to that of pure Ni. The Ni-Co alloys with up to 30% Co show pure metal-type rolling texture, while the Ni-60% Co alloy shows alloy-type texture. The rolling texture of the Ni-40% Co alloy lies in between these two extremes. The similarity of the deformation textures of pure Ni and Ni-Fe alloys can be attributed to the negligible variation of the stacking-fault energy of Ni as a function of Fe-content. The texture transition in the Ni-Co alloys has been attributed to the additional effect of the incidence of twinning caused by the sharp decrease of stacking fault energy of Ni by Co-addition [18-20].

Very few researchers have attempted to explain the deformation behaviour of nanostructured multilayered thin film materials. It indicates that Hall-Petch type dislocation pile-up models are not applicable at nanoscale layer thicknesses. Rather, deformation may involve confined layer slip, in which Orowan (hairpin) dislocation loops are confined to glide within individual layers followed by either annihilation of dislocation at interfaces or transmission of single dislocation across interfaces [21-28]. Rolling textures in nanoscale multilayered (Cu and Nb) thin films are found to differ markedly from textures observed in bulk materials. After rolling to 80% effective strain, samples with a larger initial layer thickness develop a bulk rolling texture while those with a smaller initial layer thickness display co-rotation of Cu and Nb columnar grains about the interface normal, in order to preserve the K-S orientation relations. The resulting K-S texture has (001) Nb parallel to the rolling direction and (110) Cu approximately 5 degree from the rolling direction[21].

The development of texture in deformed copper alloys depends on acroscopic localization of plastic flow induced by shear bands. Investigations carried out on CuZn30, CuNi25, and CuSn5P alloys comprised their cross-rolling, structural observations and precise measurements of texture. It has been found that, the shear bands generated during rolling, cut out in the material blocks of macroscopic size which while undergoing mutual displacement, determine its texture [29-30].

Behaviour of lead, Armco iron and steels [304 and 1009] during rolling, especially in contact zone of the billet with the roll were studied by Jacek Mazurkiewicz [31]. Data on total spread, the spread distributions over the width and the barrelling of the edges reveal that a deformational similarity that exists among the lead, Armco iron and the selected steels. Therefore, lead can be used in the modeling of hot rolling process and it is a good check of rolling design [31, 32].

3. Texture and Deformation Mechanism in Steels

Texture studies were carried out in ferrous metals subjected to various mechanical treatments/deformation like forging, rolling, torsion, etc. Large strains occur in metals when subjected to torsion testing. During torsion testing both deformation and grain boundary migration occurs. Texturing due to torsion in BCC metals has been studied at room temperature and at elevated temperature (33-36). High purity alpha-iron and Interstitial free (IF) steels deformed in torsion over the temperature range of (600-840^{o}C) was studied for texturing. The texture developed at 600^{o}C in IF steel differs from that of lower temperature textures. The addition of Niobium and Titanium also retards the development of recrystallization textures [37].

Extensive texture development was carried out by Ian Hughes [38] in different types of hot rolled and cold rolled steels to improve various mechanical properties and magnetic properties. Strict process control establishes different types of preferred orientations in the cold rolled and annealed steels which improve the magnetic properties of silicon steels and the draw abilities of low carbon stabilized steels. Hot rolling of silicon steel also yields suitable orientation thereby improving magnetic properties.

In hot rolled steels, a maximum finishing temperature of (877-860^{o}C) yield a random orientation with recrystallised equiaxed grains, whereas a minimum finishing temperature 777^{o}C yields a strong fibre texture with an elongated cold worked structure. Moreover a texture gradient is observed from the centre to the surface of the hot rolled strip [38]. This is an interesting observation, with potentially valuable applications in functionally graded materials and surface engineering.

Duplex metallic materials like Cu-Fe, duplex stainless steel, alpha-beta brass, titanium alloys, technical metallic super-conductors like Nb-Ti and Nb dispersed in copper matrix are good in rolling, forging and drawing processes, because of altered properties due to different deformation mechanisms like dislocation glide, dislocation climb, twinning, phase transformation and crack formation. In the vicinity of crack formation, crack closure, welding and refinement of the microstructure were observed to take place due to the following reasons.

If one phase is more brittle than the other, and additionally if the interface region is brittle too, then the crack propagation is limited by the most ductile component .The limitation of the crack formation and extension is the more effective when the duplex microstructure is finer.

(a) Cracks with limited length may weld under a repeated application of stress which requires both a hydrostatic component and a deviator component (roll welding). This triaxiality is promoted by the heterogeneity of the duplex structure.

(b) The fact that both crack formation and welding occur under a shear stress components leads to a refinement of the structure and the prevention of crack formation [39].

Crystallographic twinning is associated with a rigid body rotation of the crystal. Therefore the change of orientation during deformation provides information on the deformation mechanisms. Quantitative texture analysis is, therefore, an appropriate tool for the investigation of plastic deformation also in complex materials, like nitrogen alloyed duplex stainless steels [40].

4. Texturing and Deformation Mechanisms in Duplex Stainless Steels

The mechanical properties of duplex steels depend on the phase composition, the shape and arrangement of both phases as well as the textures on these phases. The duplex steel is in the ferritic state after solidification. Upon further cooling it enters the two-phase region (ferrite and austenite) in which it is being hot rolled. Hot rolling also produces preferred orientations in both phases, which also contribute to the overall mechanical anisotropy [41].

In a study made by Johan Moverare and Magnus Oden [42], the influence of elastic and plastic anisotropy on the flow behaviour of cold rolled and heat-treated sheets of duplex stainless steels was examined without prestraining. It was found that the load partitioning between the two phases depends on the loading direction. For loading in the initial rolling direction, both phases deform plastically to the same degree, while more plastic deformation occurs in the austenitic phase during loading in the transverse direction. For loading in the 45°-direction, more plastic deformation occurs in the ferritic phase. The austenitic phase has a low stacking fault energy and cannot easily cross slip during deformation. Therefore it can be inferred that a change in strain path will influence the two phases differently [42].

A strip cast material 6.97 mm in thickness was hot rolled with intermediate annealing treatments for 4-6 min at 1120^{o}C after successive individual rolling passes of 30, 19, and 41% producing a total deformation of the order of 90%. At this stage, the material contained about 60% austenite and 40% ferrite and was partially recrystallized. Annealing of hot rolled duplex steels leads to further recrystallization of the ferrite phase but not of the austenite phase. Plastic deformation of the hot rolled samples in transverse direction with respect to the hot rolling direction, results in higher hardness values for austenite than ferrite phase in as received samples as well as a greater hardening after deformation [41].

Cyclic stress-strain behaviour of duplex stainless steels is largely dependent on the applied load/strain amplitude. The difference in the elastoplastic properties between the austenite and ferrite phases as well as the load sharing between the phases, are responsible for the dependence. Lillbacka et al [43] have reported in the literature that, although the plastic deformation in SAF 2507 starts in the austenitic phase, hardness measurements after cyclic loading show that austenite is the harder of the two phases. The hardening of the austenite will lead to the transfer of plastic deformations from the austenite to the ferrite during cyclic loading.

The hardening rate of the austenite is higher than that of the ferrite. This can lead to a transition point where the austenite becomes the harder of the two

phases, if the austenite was originally the softer of the two phases. The austenite phase will always show a planar dislocation structure but with different location density. However the ferrite will show dislocation channels, walls and cells depending on the amount of plastic deformation experienced [43].

A strong grain refinement is observed with the increase in deformation of cold rolled duplex stainless steel UNS S31803 at room temperature. Also the amount of martensite α (bcc ferromagnetic) increases exponentially with deformation in highly deformed samples. Annealing at 400°C carried out after deformation promotes an increase of 4 to 6% in the ά martensite [44]. Similar observation was reported by various researchers in metastable austenitic steels [45-47].

The rolling deformation mechanisms of duplex structures differs from those of single phase materials, because the phase boundaries (PB) very effectively hinder the deformation on each phase and cause different deformation mechanisms to appear. Fine grained DSS produced by rolling or extrusion and forging followed by quenching in water, yields what are called dual phase steels where ferrite constitutes the matrix while austenite forms islands identified by its turns [48-51].

The duplex stainless steels having a fine-grained microstructure show superplastic behaviour since the grain growth is effectively retarded at high temperature due to the two- phase-aggregated microstructure. Smith and Hayden [52-54] suggested that the grain boundary sliding is the dominant mechanism for superplasticity in duplex stainless steel. It is suggested [55,56] that the dynamic recrystallization of the softer phase in a duplex microstructure, which occurs continuously during deformation, could be the dominant mechanism for superplasticity at temperatures in the range (800-1100^{o}C). This conclusion emphasizes that the deformation mechanism for superplasticity in duplex stainless steel is not exclusively grain boundary sliding which has generally considered the dominant mechanism for super plastic deformation. Even if grain boundary sliding were to be considered the controlling mechanism for superplastic deformation and the role of the dynamic recrystallization is to transform the low angle grain boundaries into high angle grain boundaries suitable for sliding [51]. Compared to single phase steels, the rolling deformation of duplex steels is much more complex, since dislocation glide, which is the most important mechanism in single phase steel is progressively hindered with increasing nitrogen content [57].

According to the Taylor theory, the accommodation of the macroscopic deformation by crystallographic glide requires the activation of five independent slip systems in every region no shears and no broadening is allowed [58]. Despite the low stacking fault energy (SFE) of the austenitic phase, due to the existence of a second phase the lower ductility of austenite and the role of planar glide no dislocation splitting and therefore no stacking faults, extensive twinning and deformation inhomogenities like shear bands could be observed. [48].

The effect of changes in strain path on the flow behaviour in duplex stainless steels was investigated by Johan J. Moverare [59]. It was found that during prestraining in the rolling direction there is a change in microstresses due to different flow behaviour in the two phases. An increase in microstress (tensile in austenite and compressive in ferrite) was observed in the transverse direction. Also, the surface macrostresses increased after prestraining due to the texture gradients observed through the thickness of the sheet. No significant changes in the texture were observed during prestraining up to 5.2% plastic strain and

therefore, differences in the anisotropic behaviour between as received and prestrained material do not originate from the crystallographic texture [59].

The Mechanical properties of both phases in duplex stainless steel have been studied in situ using neutron diffraction during mechanical loading. The main advantage of diffraction methods is the possibility to obtain separate measurements for each phase of the material. The X-ray diffraction technique is widely used for the determination of surface stresses. The advantage offered by the neutron radiation is its large penetration depth. The neutron diffraction is applied for obtaining information from the interior of the specimen.

The time-of-flight (TOF) neutron diffraction technique and self-consistent modeling were applied to investigate in situ deformation of DSS during tensile and compressive loadings. The main advantage of TOF neutron over steady-state neutron diffraction is that it allows simultaneous measurement of interplanar spacing for many hkl reflections in each studied phase, using the experimental setup.

It was reported that the ferritic phase is initially harder than the austenitic phase, i.e. the critical resolved stress of ferrite is higher than for austenite. However, the yield stresses of the phases within duplex steel are affected not only by the critical resolved stresses of the crystallite, but also by the internal stresses present within the material. In spite of the presence of the initial stresses, no significant differences in macro mechanical behaviour between tension and compression stress modes have been found [60].

Duplex stainless steel with nitrogen content of 0.32% was produced by Chandramohan et al. [61] a conventional induction furnace under normal ambient atmosphere. The samples were subsequently hot forged to various size reductions (23%-57%). The results reveal that the optimal mechanical properties were noticed for a forging deformation of 48%. Texture analysis was carried out in these samples using X-ray diffractometer by the Inverse Pole Figures (IPF) and Orientation Distribution Function (ODF) techniques and is shown in Figs. 1 - 4 for the individual phases namely ferrite and austenite. The IPF and ODF results revealed that bulk texture was weak after hot forging [61].

5. Computer Analysis of Rolling Parameters and Texture Formation

It is generally accepted that in hot deformation processes, temperature is the most significant variable, which influences product properties. Additionally, temperature also has a considerable effect on the deformation load and torque. It is therefore mandatory to ascertain the magnitude of any temperature change during the deformation and the dwell time at that temperature.

Three different approaches such as the analytical approach, the finite difference method (FDM) and the finite element method (FEM) are currently in use to calculate the temperature variation through slab thickness in the roll gap. There are quite significant differences between these approaches in the consideration of heat generation and heat loss. The analytical approach only takes into account the heat transferred between the slab and the roll by conduction [62]. The calculated temperature is rigorously correct but only under certain conditions. The FDM gives a better prediction than the analytical approach by consideration of the heat generation through the slab thickness and applying friction work to

surface elements, in addition to the conduction between the roll and the slab [10, 63]. Three-dimensional FD models are difficult to handle because remeshing facilities do not exist. The FEM is theoretically the best method because it considers all the factors, such as changing thermal properties or varying the rates of internal heat generation with position and with time and can easily incorporate remeshing [64]. The problem when employing FEMs is that the analysis takes a good deal of computer time, especially for three-dimensional deformation. For this reason analytical and FD methods are usually adopted for the design of rolling pass schedules although these yield less accurate results.

Significant temperature gradient exists between the surface and the centre of the heated slab. For commercial pure aluminium slab heated to 500^{o}C the surface temperature is about 75^{o}C lower than the slab centre temperature. Due to this temperature gradient between surface and the centre, the material flow behaviour will be affected considerably. The value of flow stress at the surface will be much higher than the flow stress at the slab centre. The material at the slab centre flows outward easily, and little material slides to the edge, leading a convex lateral profile [65].

Texture development during grain growth has been studied mainly through statistical modeling and Monte Carlo (MC) simulations. Initially Hilert [66] developed a statistical model of grain growth. Then Abbruzzese and Lucke [67] studied the interactions between two texture components by extending Hilert's statistical model of grain growth. For simplicity, they considered two types of grain orientations (or texture components) A and B with three types of grain boundaries (A-A, B-B, and A-B). Accounting for an isotropy only in the boundary mobility, with high mobility for A-B and low mobility for A-A and B-B boundaries, they have shown that the minority component should grow at the expense of the majority component, leading to oscillations in some volume fractions of the two texture components. The same type of phenomenon was also observed by Mehnert and Klimanek [68, 69] and by Ivasishin et al. [70] in their Monte Carlo simulations.

Evolution of a single texture component (A) was studied by Abbruzzese and Lucke [67], in a matrix of randomly oriented grains (B) [71]. In Novikov's statistical analysis, both A-B and B-B boundaries were assumed to have high energy and high mobility, and it was concluded that the fraction of textured grains (in the case of A grains) decreases until their initial average size was much larger than that of the matrix B grains. Hwang et al. [72] used MC simulations to study a system similar to Novikov's, but they allowed for anisotropy only in boundary energy. They observed a marked growth of the texture component even when the texture grains did not have an initial size advantage. Rollet [73] also investigated evolution of a single cube textured component in the matrix of randomly oriented grains using the MC method. He employed two sets of functions for misorientation dependence of mobility and energy, and found that the texture evolution was sensitive to mobility function but not to the energy function.

An online program called CROWN has been developed for temperature, profile and shape control in plate and strip mills by Mantyla P. et al. [74]. The experimental data and the simulation data were verified with the plate mean temperatures, plate profiles and work roll profiles in production mill. CROWNON is another online program, which has been developed to improve the existing pass schedule. If the mills is equipped with some kind of profile and shape meter and adaptive control system can be constructed where CROWNON calibrates simple on-line shape and

profile equations against measured shapes and profiles. The decision can be made as to which kind of on-line process control is going to be used in the actual case example recalculation of the schedule, roll bending or selective roll cooling. The system has decreased the number of passes, improved the yield and has provided the possibility of rolling thin wide plates [74].

Upon continuous service, rollers are subjected to deviate from its alignment. This alignment correction becomes a laborious job and even time consuming. In order to overcome this difficulty the roller straightening process was attempted using computer simulation and the whole process (from entry to product exit) was simulated. The various mathematical models considered the variables like flexibility, radii and current positions of the rollers, product deformation, material properties of the straightened product. Results of the simulations were related to some experimental data and a sufficient compatibility was observed [75].

6. Factors Affecting Textures Evolution

Many factors affect texture evolution during the grain growth. These are number of texture components, degree of texturing, initial volume fractions, grain sizes, size distributions of different texture components, anisotropy in grain boundary energy and mobility. In addition, the spatial distribution of the texture component in the initial microstructure is also important because the spatial distribution affects the misorientation directly and the misorientation distribution function (MDF).

Independent of texture evolution, extensive work has been done in modeling the effect of anisotropy in the boundary energy and mobility on the morphology of polycrystalline microstructure and the kinetic coarsening during the grain growth [76-78]. It has been demonstrated [77,78] that starting with either a component texture or a random texture anisotropy, boundary mobility plays a small role, while boundary energy strongly modifies both morphology and the kinetics of grain growth. Even though all the factors considered affect the texture evolution it is found that the key parameter that controls the texture evolution is the grain boundary energy density.

Clustering of textured grains is inevitable during coarsening. The degree of clustering depends on the initial dispersion of the textured gains. Clustering causes an increase in the fraction of low angle boundaries in a system and hence alters the misorientation distribution function (MDF). As a consequence initial microstructure of different degrees of clustering of textured grains is associated with different time evolutions of (MDF) and hence has different grain growth kinetics [79]. An analytical model for predicting crystallographic textures and the final grain size during primary static recrystallization of metals using texture components was developed by Dierk Raabe [80]. The first equation describes the thermally activated nucleation and growth processes for the expanded (free) volume for a particular couple of a deformed and recrystallizing texture component and the second equation is used for calculating the constrained (real) volume for that couple which corrects the free volume for those portions of the deformed component which were already swept. This new method is particularly developed for the fast and physically based process simulation of recrystallization textures with respect to processing and applied to the primary recrystallization of low carbon steels [80].

$$\Delta V_{ij}^{\exp} = N_{ij} \frac{4}{3} \prod \left(\left(\left\langle r_{ij} \right\rangle + \left\langle r_{ij} \right\rangle \right)^3 - \left\langle r_{ij} \right\rangle^3 \right) \quad (1)$$

$$N_{ij} = N_{0ij} \left\langle \exp\left(- Q_{ij}^{nuc} / k_B T \right) \right\rangle \Delta t \quad (2)$$

$$\left\langle \Delta r_{ij} \right\rangle = m_{0ij} \left\langle \exp\left(- Q_{ij}^{mob} / k_B T \right) \right\rangle P_j \Delta t \quad (3)$$

where

$\left\langle \exp\left(- Q_{ij}^{nuc} / k_B T \right) \right\rangle$ - Thermal activation term of the grain boundary for a nucleation texture component *i* that grows into texture component *j*.

$\left\langle \exp\left(- Q_{ij}^{mob} / k_B T \right) \right\rangle$ - Thermal activation term for recrystallization mobility for a recrystallizing texture component *i* in deformed texture component *j*.

$$\Delta V_{ij}^{RX} = \left(X_{0j}^{def} - \sum_{n=1}^{n_{\max}} X_{nj}^{RX} \right) \Delta V_{ij}^{\exp} \quad (4)$$

7. Occupational Health and Safety

In the present day industrial scenario, health and safety related issues are becoming mandatory. The workspace in which a thermomechanical treatment is carried out is no way exempted from this issue. In order to have an idea on the effect of heat, fumes, carbon monoxide emission, work shift change, etc. which are commonly prevailing in the mechanical processing industries like smelting units, Ferro alloy plants, Chromium exposing units, welding units, etc. literatures related to health and safety are discussed below.

A study on the occupational exposure and cancer incidence among workers from an aluminum smelter in western Norway revealed a positive association between bladder cancer and PAH exposure. The short-term workers showed a statistically significant excess of lung cancer [81]. A study on the Mortality from cardiovascular diseases and sudden death in ferroalloy plants revealed that increased mortality from sudden death among the FeMn/SiMn furnace workers is associated with work exposures (manganese and possibly carbon monoxide and heat). The increasing mortality from hypertension-related diseases with increased duration of work in furnace workers are associated with common furnace work conditions such as heat, psychosocial stress, shift work, noise and carbon monoxide [82]. A study on the associations between asphalt fumes and work shift changes in lung function and symptoms among workers exposed to asphalt fumes revealed that no consistent association exists between an acute reduction in lung function and exposure to asphalt fumes [83].

Field surveys in selected industries at United States were conducted to characterize workers' exposures to hexavalent chromium-containing airborne particulate and to evaluate existing technologies for controlling these exposures. The surveys concluded that, in many of the evaluated processes, Chromium exposures at or below the current level are achievable. However, for some processes, it is unclear whether controlling exposures to this range is consistently achievable without respirator use [84]. A study on the risk of lung cancer due to

mild steel and stainless steel welding revealed that standardized incidence ratio (SIR) for lung cancer was increased among the welders [SIR 1.35, 95% confidence interval (95% CI) (1.06–1.70)]. Among the stainless steel welders, the risk increased significantly with increasing accumulative welding particulate exposure, while no exposure–response relation was found for mild steel welders [85].

Exposure to airborne metals in the manufacture and maintenance of hard metal and stellite blades show that workers grinding hard metal blades are exposed to high levels of airborne cobalt even when airborne total dust concentrations are low. The respirable portion of total dust was found to be high, and the total concentrations correlated well with the cobalt concentrations. To reduce workers exposure to cobalt, it is recommended that grinding machines should be enclosed and equipped with local exhausts. Use of coolants that dissolve less cobalt is also recommended [86].

From the above discussion it is prudent that health risks exist on a short term or in a long term due to the exposures like chromium, cobalt, fumes, heat, noise, etc. in a metal working industry. Therefore to aim for a sustainable growth, while carrying out a thermomechanical treatment, an internationally proven standard which addresses Occupational health and safety (OHSAS 18001:2007) shall be practiced.

8. Summary and Suggestions

In this overview, the initial processing methods (Concast or chill casting), influence of alloying content on Stacking fault energy, different mechanisms of deformation in Nanostructured multilayer, texture and morphology of grains across the cross section of rolled billets, study of materials using Neutron diffraction / XRD and design of roll pass schedules, profiles, shape control, etc. using various theoretical methods like FEM, FDM, etc. has been discussed in detail. Progress in new approaches to study the relative roles of metallurgical factors (anisotropy, grain boundary) has also been mentioned. It is evident that texture studies on nitrogen alloyed duplex stainless steel offer great possibility for commercialization and for different applications.

The review has brought out that sufficient studies have been carried out in optimizing the rolling parameters like rolling temperature, rolling speed, roll temperature, friction, and ratio of thickness to the contact length in the roll gap. Among these rolling parameters, rolling temperature has the greatest influence while the roll temperature and roll speed have little influence on the microstructure and texture. The magnitude of temperature change during deformation has been analysed theoretically using FEM and FDM methods. However, to have better control over the preferred texture development, experimental study and quantitative analysis is very much required. Future research should be focused on the study of texture development in nitrogen alloyed duplex stainless steels by varying the rolling temperature i.e. cold warm and hot conditions along with the various size reductions. Occupational health and safety practices can be implemented during the erection of rolling mill as well as rolling process. Attempts in these areas are in progress in the author's laboratory.

Acknowledgment

The authors are grateful to AICTE (All India Council for Technical Education) for funding this research project. National Facility of Texture and Orientation Imaging Microscopy - Department of Science and Technology, India at IIT-Bombay and Defence Metallurgical Research Lab, Hyderabad support this work. The authors are grateful to m/s Auto Shell casts pvt ltd and m/s Commando Engineers, Coimbatore, India for supplying and processing the DSS material.

References

1. Panda, A.K.; Ray, P.K.; and Ganguly, R.I. (2000). Effect of thermomechanical treatment parameters on mechanical properties of duplex ferrite–martensite structure in dual phase steel. *Materials Science and Technology*, 16(6), 648-656.
2. Seijiro Maki; Minoru Ishiguro; and Hiroyasu Makino. (2006). Thermo-mechanical treatment using resistance heating for production of fine-grained heat-treatable aluminum alloy sheets. *Journal of Materials Processing Technology*, 177(1-3), 444-447.
3. Zheng, K.Y.; Dong, J.; Zeng, X.Q.; and Ding, W.J. (2007). Effect of Thermo-mechanical treatment on the mechanical properties of a Mg-6Gd-2Nd-0.5Zr alloy. *Material Science and Engineering: A*, 454, 314-321.
4. Bron, D.I.; Rakhshadt, A.G.; and Levites, I.I. (1963). Effect of thermo-mechanical treatment on the fatigue resistance of 55KhGR steel. *Metal Science and Heat Treatment*, 5(4), 210-211.
5. Dmitry Eskin, G.; Nikolay Belov, A.; and Andrey Aksenov, A. (2005). *Multicomponent Phase Diagrams: Applications for Commercial Aluminium Alloys.* Harbound Publication.
6. Robert Gunn, N. (1997). *Duplex stainless steels microstructure, properties and applications.* Abington Publishing.
7. ASM Specialty Handbook. (1994). *Stainless Steel.* ASM International.
8. Verma, B.B.; Atkinson, J.D.; and Kumar, M. (2001). Study of fatigue behaviour of 7475 aluminum alloy. *Bulletin of Material Science*, 24(2), 231-236.
9. Duan, X.; and Sheppard, T. (2002). Influence of forming parameters on static recrystallization behaviour during hot rolling aluminium alloy 5083. *Modelling and Simulation in Material science and Engineering*, 10, 363-380.
10. Sheppard, T.; and Wright, D.S. (1981). Parameters affecting lateral deformation in slabbing mills. *Metals Technology*, 8, 46-57.
11. Raghunathan, N.; and Sheppard.T. (1989). Microstructural development during annealing of hot rolled Al-Mg alloys. *Material Science Technology*, 5, 542-547.
12. Sheppard, T.; and Duan, X. (2002). A new spread formula for hot flat rolling of aluminium alloys. *Modelling and Simulation in Materials Science and Engineering*, 10(6), 597-610.
13. Rdzawsky and Sadkowski, A. (1992). New approach to developing a rolling technology. *Journal of Material Processing Technology*, 34, 287-294.
14. Liu, W.C.; Zhai, T.; and Morris, J.G. (2004). Texture evolution of continuous cast and direct chill cast AA 3003 aluminum alloys during cold rolling. *Scripta Materialia*, 51(2), 83-88.

15. Liu, W.C. and Morris, J.G. (2002). Kinetics of the formation of the β fiber rolling texture in continuous cast AA 5xxx series aluminum alloys. *Scripta Materialia*, 47, 743-748.
16. Liu, W.C.; and Morris, J.G. (2003). Comparison of the texture evolution in cold rolled DC and SC AA5182 aluminum alloys, *Material Science Engineering A*339,183-193.
17. Zhao, Y.M.; Liu, W.C.; and Morris, J.G. (2004). Quantitative analysis of texture evolution of cold-rolled direct-chill-cast and continuous-cast AA5052 and A5182 aluminum alloys during isothermal annealing. *Metallurgical and Materials Transactions A*, 35A (11), 3613-3629.
18. Ray, R.K. (1995). Rolling textures of pure nickel, nickel-iron and nickel-cobalt alloys. *Acta metallurgica et Materialia*, 43(10), 3861-3872.
19. Caleyo, F.; Baudin, T.; Penelle, R.; and Venegas, V. (2001). EBSD study of the development of cube recrystallization texture in Fe–50%Ni. *Scripta Materialia*, 45(4), 413-420.
20. Branger, V.; Mathon, M.H.; Baudin, T.; and Penelle, R. (2000). "in-situ" neutron diffraction study of the cube crystallographic texture development in Fe53%-Ni alloy during recrystallization. *Scripta Materialia*, 43(4), 325-330.
21. Peter Anderson, M.; John Bingert, F.; Amit Misra; and John Hirth, P. (2003). Rolling textures in nanoscale Cu/Nb multilayers. *Acta Materialia*, 51, 6059-6075.
22. Misra, A.; Hirth, J.P.; and Kung, H. (2001). Single-dislocation-based strengthening mechanisms in nanoscale metallic multilayers. *Philosophical Magazine A*, 82(16), 2935-2951.
23. Kreidler, E.R.; and Anderson, P.M. (1996). Orowan-based deformation model for layered metallic materials. *MRS Symposium Proceedings 434, Materials Research Society:* Warrendale, PA, 159-170.
24. Anderson, P.M.; Foecke, T.; and Hazzledine, P.M. (1999). Dislocation-based deformation mechanisms in metallic nanolaminates. *Materials Research Society Bulletin*, 24(2), 27-33.
25. Nix, W.D. (1998). Yielding and strain hardening of thin metal films on substrates. *Scripta Materialia*, 39(4), 545-554.
26. Rao, S.I.; and Hazzledine, P.M. (2000). Atomistic simulations of dislocation-interface interactions in the Cu-NI multilayer system. *Philosophical Magazine A*, 80(9), 2011-2040.
27. Hoagland, R.G.; Mitchell, T.E.; Hirth, J.P.; and Kung, H. (2002). On the strengthening effects of interfaces in multiplayer FCC metallic composites. *Philosophical magazine A*, 82(4), 643-664.
28. Misra, A.; and Kung, H. (2002), *Los Almos National Laboratory*, unpublished work.
29. Stalony-Dobrzanski, F.; and Bochniak, W. (2004). Roll of shear bands in forming the texture image of deformed copper alloys. *Integrated study of basis of plastic deformation of metals*, Lancut, Poland.
30. Engler, O. (2001). Recrystallization textures in copper manganese alloys. *Acta Materialia*, 49(7), 1237-1247.
31. Jacek Mazurkiewicz; and Piotr Myszkowski. (1991). Similarity in the deformation of lead and steel in the hot-rolling process. *Journal of Materials Processing Technology*, 26, 23-33.

32. Shida, S. (1979). Simulation of hot rolling of steel using lead. *Translation ISIJ*, 19, 700-705.
33. De Kazinczy, F.; and Backofen, W.A. (1960). Influence of hot rolling condition shipping on brittle fracture in steel plate. *Progress report of the project SR 147, Dept. of Navy, American Bureau of shipping*, 1-32.
34. Toth, L.S.; Lendvai, J.; Kovacs, I.; and Albert, B. (1985). The plastic behaviour of <100> and <111> textured polycrystalline metals during simultaneous torsion and extension. *Journal of Materials Science*, 20(11), 3983-3987.
35. Stout, M.G.; and Staudhammer, K.P. (1984). Biaxial deformation of 70-30 brass: Flow behaviors, texture, microstructures. *Metallurgical and Materials Transactions A*, 15(8), 1607-1612.
36. Goes, B.; Martín-Meizoso, A.; Gil-Sevillano, J.; Lefever, I.; and Aernoudt, E. (1998). Fragmentation of as-drawn pearlitic steel wires during torsion tests. *Engineering Fracture Mechanics*, 60(3), 255-272.
37. Baczynski, J.; and Jonas, J.J. (1998). Torsion textures produced by dynamic recrystallization in alpha-iron and two interstitial–free steels. *Metallurgical and Materials Transactions A*, 29A, 447-462.
38. Ian Hughes, F. (1971). The effect of finishing temperature on the texture and structure of hot rolled 1 pct Si steel. *Metallurgical Transactions B*, 2, 929-936.
39. Foct, J., Akdut, N. and Gottstein, G. (1992). Why are duplex microstructures easier to form than expected? *Scripta Metallurgica et Materialia*, 27 (8), 1033-1038.
40. Akdut, N.; and Foct, J. (1995). Phase boundaries and deformation in high nitrogen duplex stainless steels I.–Rolling texture development. *Scripta Metallurgica et Materialia*, 32(1), 103-108.
41. Ul-Haq., A.; Weiland, H.; and Bunge, H.J. (1994). Textures and microstructures in duplex stainless steel. *Material Science and Technology*, 10, 289-298.
42. Johan Moverare, J.; and Magnus Oden. (2002). Influence of elastic and plastic anisotropy on the flow behavior in a duplex stainless steel. *Metallurgical and Materials Transactions A*, 33(1), 57-71.
43. Lillbacka, R.; Chai, G.; Ekh, M.; Liu, P.; Johnson, E.; and Runesson, K. (2007). Stress-strain behaviour and load sharing in duplex stainless steels: Aspects of modeling and experiments. *Acta Materialia*, 55(16), 5359-5368.
44. Tavares, S.S.M.; da Silva, M.R.; Paradal, J.M.; Abreu, H.F.G.; and Gomes, A.M. (2006). Micro structural changes produced by plastic deformation in UNS S31803 duplex stainless steel. *Journal of Materials Processing Technology*, 180(1-3), 318-322.
45. Toshihiko Takemoto; Yasushi Murata; and Teruo Tanaka. (1990). Effects of alloying elements and thermo-mechanical treatments on mechanical and magnetic properties of Cr-Ni austenitic stainless steel. *ISIJ International*, 30(8), 608-614.
46. Gauzzi, F.; Montanari, R.; Principi, G.; and Tata, M.E. (2006). AISI 304 steel: anomalous evolution of martensitic phase following heat treatments at 400°C, *Materials Science and Engineering A*, 438-440, 202-206.
47. Gauzzi, F.; Montanari, R.; Principi, G.; Perin, A.; and Tata, M.E. (1999). Martensite formation during heat treatments of AISI 304 steel with biphasic structure. *Materials Science and Engineering A*, 273-275, 443-447.

48. Akdut, N.; and Foct, J. (1995). Phase boundaries and deformation in high nitrogen duplex stainless steels-II. Analysis of deformation mechanisms by texture measurements in X2CrNiMo 225(1.4462). *Scripta Metallurgica et Materialia*, 32(1), 109-114.
49. Chandramohan, P.; Mohamed Nazirudeen, S.S.; and Srivatsavan, R. (2006). The effect of nitrogen solubility, heat treatment and hot forging on 0.15% N duplex stainless steels. *International Journal of Materials and Product technology (IJMPT)*, Inderscience Publication, UK, 25(4), 281-296.
50. Chandramohan, P.; Mohamed Nazirudeen, S.S.; and Ramakrishnan, S.S. (2007). Studies on hot forging of nitrogen alloyed duplex stainless steels. *Journal of Materials Science and Technology*, 23(1), 111-117.
51. Young Han, S.; and Soon Hong, H. (1997). The effects of thermo-mechanical treatments on superplasticity of Fe-24Cr-7Ni-3Mo-0.14 N duplex stainless steel. *Scripta Materialia*, 36(5), 557-563.
52. Hayden, H.W.; Floreen, S.; and Goodell, P.D. (1972). The deformation mechanisms of superplasticity. *Metallurgical and Materials Transactions B*, 3(4), 833-842.
53. Hayden, H.W.; and Floreen, S. (1970). The influence of martensite and ferrite on the properties of two-phase stainless steels having micro duplex structures. *Metallurgical and Materials Transactions B*, 1(7), 1955-1959.
54. Smith, C.I.; Norgate, B.; and Ridley, N (1976). Superplastic deformation and cavitation in a microduplex stainless steel. *Metal Science*, 10, 182-188.
55. Maehara,Y.; and Ohmori, Y. (1987). Microstructural change during superplastic deformation of delta-ferrite/austenite duplex stainless steel. *Metallurgical and Materials Transactions A,* 18 (5), 663-672.
56. Yasuhiro Maehara. (1991). High strain rate superplasticity of a 25 Wt Pct Cr-7 Wt Pct Ni-3 Wt Pct Mo-0.14 Wt Pct N duplex stainless steel. *Metallurgical and Materials Transactions A*, 22(5), 1083-1091.
57. Akdut, N.; and Foct, J. (1993). Cleavage-like fracture of austenite in duplex stainless steel. *Scripta Metallurgica et Materialia*, 29(2),153-158.
58. Taylor, G.I. (1938). Plastic strain in metals. *Journal of the Institute of metals*, 62, 307-324.
59. Johan Moverare J.; and Magnus Oden. (2002). Deformation behaviour of a prestrained duplex stainless steel. *Materials Science and Engineering A*, 337(1-2), 25-38.
60. Dakhaloui, R.; Baczmanski, A.; Braham, C.; Wronski. S.; and Oliver, E.C. (2006). Effect of residual stresses on individual phase mechanical properties of asuteno-ferritic duplex stainless steel. *Acta Materialia*, 54(19), 5027-5039.
61. Chandramohan, P.; Mohamed Nazirudeen, S.S.; and Ramakrishnan, S.S. (2008). Studies on production and thermomechanical treatment of 0.32% nitrogen alloyed duplex stainless steel. *Journal of Materials Engineering and Performance*, 17(2), 271-279.
62. Bradley, B.F.; Cockett, W.A.; and Peel, D.A. (1970). Transient temperature behaviour of aluminium during rolling and extrusion. Proceeding conference on mathematical models in metallurgical process development, *Iron and Steel Institute Publication* 123, 79-90.

63. Hand, R.J; Foster, S.R.; and Sellars, C.M. (2000). Temperature changes during hot plain strain compression testing. *Materials Science and Technology*, 16(4), 442- 450.
64. Dawson, P.R. (1984). A model for the hot or warm forming of metals with special use of deformation mechanism maps. *Mechanical science*, 26 (4), 227-244.
65. Duan, X.; and Sheppard, T. (2001). Prediction of temperature evolution by FEM during multi-pass hot flat rolling of aluminium alloys. *Modelling and Simulation in material science and engineering*, 9, 525-538.
66. Hillert, M. (1965). On the theory of normal and abnormal grain growth. *Acta Metallurgica* 13(3), 227-238.
67. Abbruzzess, G.; and Lucke, K. (1986). A theory of texture controlled grain growth: I. Derivation and general discussion of the model. *Acta Metallurgica* 34(5), 905-914.
68. Mehnert, K.; and Klimanek, P. (1996). Monte Carlo simulation of grain growth in textured metals using anisotropic grain boundary mobilities. *Computational material science*, 7(1), 103-108.
69. Mehnert, K.; and Klimanek, P. (1997). Grain growth in metals with strong textures: Three-dimensional Monte Carlo simulations, *Computational material science*, 9(1), 261-266.
70. Ivasishin, O.M.; Shevchenko, S.V.; Vasiliev, N.L.; and Semiatin, S.L. (2003). 3D Monte-Carlo simulation of texture-controlled grain growth. *Acta Materialia*, 51(4), 1019 – 1034.
71. Novikov, V.Yu. (1999). Texture development during grain growth in polycrystals with strong preferred orientation. *Acta Materialia*, 47(6), 1935-1943.
72. Hwang, N.M.; Lee, B.J.; and Han, C.H. (1997). Texture evolution by grain growth under a system of anisotropic grain boundary energy. *Scripta Materialia*, 37(11), 1761-1767.
73. Rollett, A.D. (2002). Texture development dependence on grain boundary properties. *Material science forum*, 408-412, 251-256.
74. Mantyla, P.; Korhonen, R.; and Jonsson, N.G. (1992). Improved thickness and shape accuracy with advanced pass scheduling in plate rolling. *Journal of Material Processing Technology*, 34, 255-263.
75. Mischke, J.; and Jonca, J. (1992). Simulation of the roller straightening process. *Journal of Material Processing Technology*, 34, 265-272.
76. Holm, E.A.; Hassold, G.N.; and Miodownik, M.A. (2001). On misorientation distribution evolution during anisotropic grain growth. *Acta Materialia*, 49(15), 2981-2991.
77. Kazaryan, A.; Wang, Y.; Dregia, S.A.; and Patton, B.R. (2002). Grain growth in anisotropic systems: comparison of effects of energy and mobility. *Acta Materialia*, 50(10), 2491-2502.
78. Upmanyu, M.; Hassold, G.N.; Kazrayn, A.; Holm, E.A.; Wang, Y.; Patton, B.R.; and Srolovitz, D.J. (2002). Boundary mobility and energy anisotropy effects on microstructural evolution during grain growth. *Interface Science*, 10(2-3), 201-216.

79. Ma, N.; Karzaryan, A.; Dregia, S.A.; and Wang, Y. (2004). Computer simulation of texture evolution during the grain growth effect of boundary properties and initial microstructure. *Acta Materialia*, 52(13), 3869-3879.
80. Dierk Raabe. (2007). A texture-component Avrami model for predicting recrystallization textures, kinetics and grain size. *Modelling and Simulation in Materials Science and Engineering*, 15, 39-63.
81. Ronneberg, A.; Haldorsen, T.; Romundstad, P.; and Andersen, A. (1999). Occupational exposure and cancer incidence among workers from an aluminum smelter in western Norway. *Scandinavian Journal of Work Environment and Health*, 25(3), 207-214.
82. Hobbesland, A.; Kjuus, H.; and Thelle. D.S. (1997). Mortality from cardiovascular diseases and sudden death in ferro-alloy plants. *Scandinavian Journal of Work Environment and Health*, 23(5), 334-341.
83. Gamble, J.F; Nicolich, M.J.; Barone. N.J.; and Vincent, W.J. (1999). Exposure-response of asphalt fumes with changes in pulmonary function and symptoms. *Scandinavian Journal of Work Environment and Health*, 25(3), 186-206.
84. Blade, L.M.; Yencken, M. Story; Wallace, M.E.; Catalano, J.D.; Khan, A.; Topmiller, J. L.; Shulman, S. A.; Martinez, A.; Crouch, K. G.; Bennett, J. S. (2007). Hexavalent chromium exposures and exposure-control technologies in American enterprise. *Journal of Occupational and Environmental Hygiene*, *Philadelphia*, 4(8), 596-618.
85. Sorensen, A.R.; Thulstrup, A.M.; Hansen, J.; Ramlau-Hansen, C.H.; Meersohn, A.; Skytthe, A.; and Bonde, J.P. (2007). Risk of lung cancer according to mild steel and stainless steel welding. *Scandinavian Journal of Work Environment and Health*, 33(5), 379-386.
86. Linnainmaa., M.; Kangas., J.; and Kalliokoski., P.. (1996). Exposure to airborne metals in the manufacture and maintenance of hard metal and stellite blades. *American Industrial Hygiene Association Journal*, 57(2), 196–201.

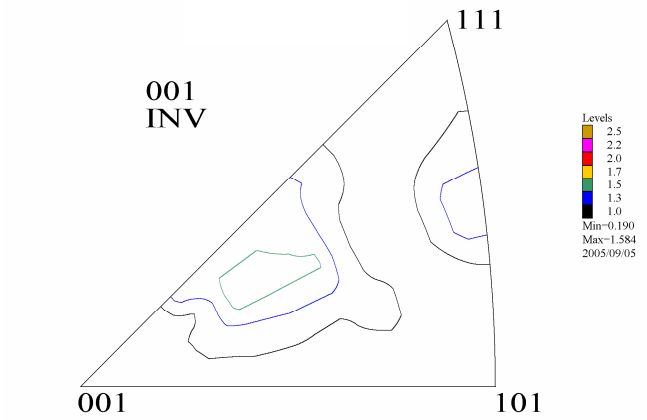

Fig. 1. IPF of Ferrite Phase in 48% Forged DSS Alloy with 0.32% N.

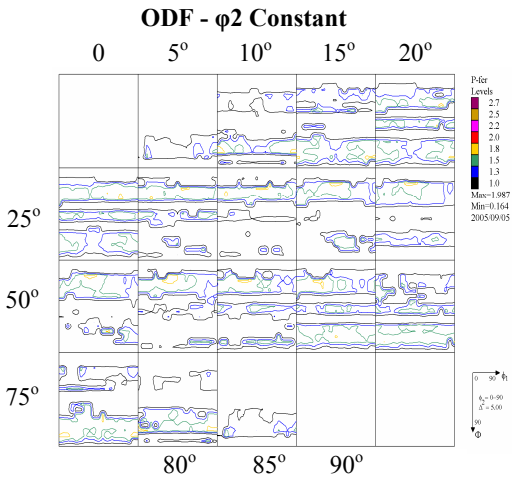

Fig. 2. ODF of Ferrite Phase in 48% Forged DSS Alloy with 0.32% N.

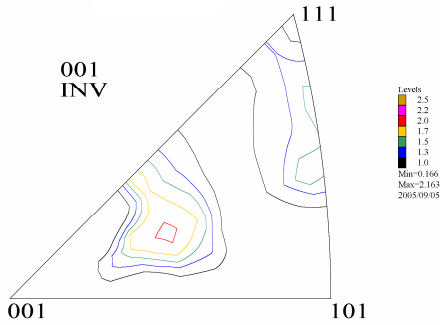

Fig. 3. IPF of Austenite Phase in 48% Forged DSS Alloy with 0.32% N.

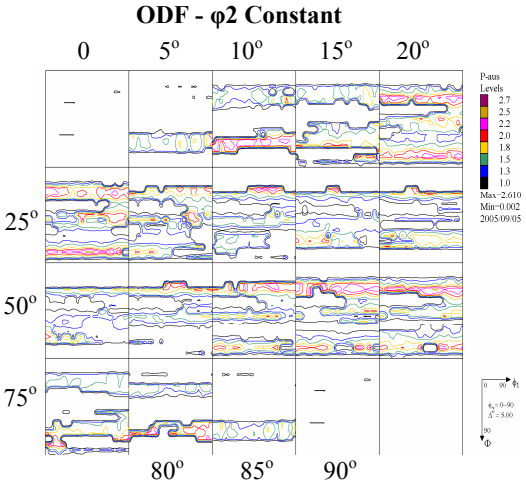

Fig. 4. ODF of Austenite Phase in 48% Forged DSS Alloy with 0.32% N.